*Int. J. Pres. Ves. & Piping* **30** (1987) 77–86

# An Investigation of the Brazier Effect of a Cylindrical Tube under Pure Elastic–Plastic Bending

L. C. Zhang and T. X. Yu

Department of Mechanics, Beijing University, Beijing,
People's Republic of China

(Received 8 March 1987; accepted 17 March 1987)

*ABSTRACT*

*The Brazier effect of originally straight cylindrical tubes under pure elastic–plastic bending is investigated by the deformation theory based on some deformation assumptions agreeing with numerous experiments. The expressions for bending moment and flattening ratio in terms of curvature are finally obtained.*

## NOMENCLATURE

| | |
|---|---|
| $A_0$, $A_f$ | Original and current flow areas of tube, respectively |
| $E$ | Young's modulus |
| $K$ | Axial curvature of tube |
| $M$ | Bending moment |
| $n$ | Material constant defined by eqn (8) |
| $R$ | Radius of original middle surface of circular tube |
| $s$, $t$ | Natural coordinates, as shown in Figs 1 and 2 |
| $T$ | Thickness of tube wall |
| $U$ | Strain energy per unit length of tube, defined by eqn (7) |
| $w$ | Normal displacement of middle surface of tube, as shown in Fig. 3. |
| $x$, $y$, $z$ | Cartesian coordinates, as shown in Figs 1 and 3 |
| $\varepsilon_s$, $\varepsilon_z$ | Circumferential and axial strain components, respectively |
| $\bar{\varepsilon}$, $\bar{\sigma}$ | Effective strain and effective stress, respectively |
| $\zeta$ | Flattening ratio of cross-section of tube |



*Int. J. Pres. Ves. & Piping* 0308-0161/87/$03·50 

$\nu$ Poisson's ratio
$\rho_s$, $\rho_z$ Circumferential and axial radii of curvature, respectively
$\sigma_s$, $\sigma_z$ Circumferential and axial stress components, respectively
$\omega_1$, $\omega_2$ Notations defined by eqns (13a, b)

## INTRODUCTION

The flattening of elastic tubes under pure bending has been a focus of much attention over many decades since Brazier first studied this problem in 1927.[1] For instance, Reissner,[2] Seide and Weingarten[3] and others have made contributions in this area, while the phenomenon of the flattening of elastic tubes under bending has been usually called the *Brazier effect* after Brazier's work. Since it is of great significance to chemical and nuclear power plants which possess complicated pipelines,[4] Gerber[5] studied this effect by taking the plastic properties into consideration, although his investigation was relatively elementary. Recently, numerous workers (e.g. Refs 6–9) have reported their experiments on this phenomenon and provided some elementary analyses to fit the experimental results. These results form the basis for the further theoretical studies of the problem. The main points are:

(1) the flattening of cross-sections of a tube becomes more severe as the maximum surface strain of the tube increases;
(2) the reduction of the diameter perpendicular to the vector of the bending moment is always almost equal to the elongation of that parallel to the vector;
(3) the measurements in dynamic tests show that the moment at which the surface strain reaches its maximum value is very close to the moment when the applied load arrives at its peak unless the tube has been broken before this point;
(4) the maximum surface strain of the tube with diameter between 29·8 mm and 165·2 mm varies from 0·002 to 0·103 5.

The well-known energy method is employed in the present paper. Formulae to show the flattening collapse of arbitrary cylindrical tubes with one symmetric plane under elastic–plastic pure bending are derived. As a special example, a circular tube is investigated in detail. Some valuable results, such as the expressions of bending moment and the flattening ratio of cross-section of the tube in terms of the radius of curvature, are obtained. The analyses in this paper are based on the following assumptions which agree with the experimental results stated above:

(1) every cross-section of the tube remains in a plane during bending;
(2) the material of the tube is incompressible, and the effective stress and effective strain are related by the power work-hardening law;

(3) the problem is considered as a static one and the strain is small in comparison with unity;
(4) local unloading in the tube wall during bending is neglected.

Hence, Ilyushin's simple loading theorem is satisfied, and the deformation theory can be employed.

## ANALYSES

Attention is restricted to pure in-plane bending only, thus the cross-section of the tube should be symmetrical with respect to the plane to which the bending moment vector is perpendicular. Figures 1(a) and (b) show the

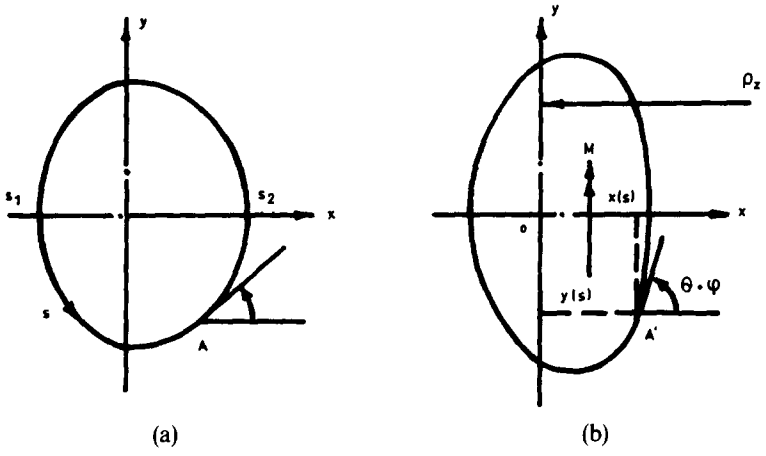


**Fig. 1.** Cross-section of the middle surface: (a) undeformed; (b) deformed.

configurations of the middle surfaces of the tube before and after deformation, respectively. The flattened cross-section is described by the Cartesian coordinates $(x(s), y(s))$, where $s$ is the circumferential arc length measured along the undeformed middle surface. We need consider only the half of the cross-section defined by $s_1 \leq s \leq s_2$ due to the symmetry of the problem. The angle and the circumferential strain of the middle surface, $\varphi(s)$ and $\mathring{\varepsilon}(s)$, respectively, are introduced.

From Fig. 1 the following useful relationships for the deformed middle surface can be derived:

$$\mathrm{d}x/\mathrm{d}s = (1 + \mathring{\varepsilon}_s)\cos(\theta + \varphi) \tag{1}$$

$$\mathrm{d}y/\mathrm{d}s = (1 + \mathring{\varepsilon}_s)\sin(\theta + \varphi) \tag{2}$$

where $\theta = \theta(s)$ is an angle given by the geometry of the undeformed cross-section. In addition, the axial strain of the middle surface, $\mathring{\varepsilon}_z$, can be expressed as

$$\mathring{\varepsilon}_z = \frac{x}{\rho_z} - 1 \tag{3}$$

where $\rho_z$ is the radius of curvature of the current centroid line of the tube.

On the other hand, an infinitesimal segment of the undeformed cross-section can be defined by the circumferential arc length, d$s$, and the distance from the middle surface, $t$ (see Fig. 2). After deformation, the length of this

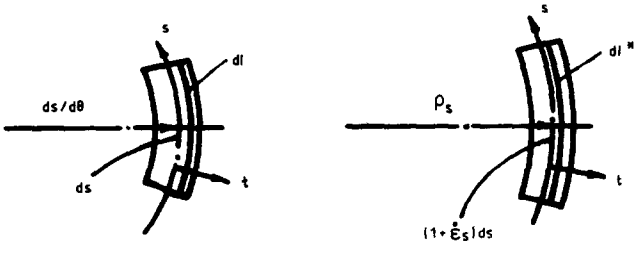


(a) (b)

**Fig. 2.** Circumferential deformation of an infinitesimal segment of tube wall: (a) undeformed; (b) deformed.

arc becomes $(1 + \mathring{\varepsilon}_s)\,\mathrm{d}s$. Since the thickness of the tube wall remains constant due to the assumption of incompressibility of the material, the axial strain of a tube fibre located at $(s,t)$ becomes

$$\varepsilon_z = \mathring{\varepsilon}_z(s) + \frac{t}{\rho_z}\sin(\theta + \varphi) \tag{4}$$

To derive the expression of the circumferential strain, $\varepsilon_s(s,t)$, note that the radius of curvature in direction $s$, $\rho_s$, of the middle surface can be expressed as

$$\rho_s = \frac{\left[\left(\dfrac{\mathrm{d}y}{\mathrm{d}s}\right)^2 + \left(\dfrac{\mathrm{d}x}{\mathrm{d}s}\right)^2\right]^{3/2}}{\dfrac{\mathrm{d}y}{\mathrm{d}s}\dfrac{\mathrm{d}^2x}{\mathrm{d}s^2} - \dfrac{\mathrm{d}^2y}{\mathrm{d}s^2}\dfrac{\mathrm{d}x}{\mathrm{d}s}} \tag{5a}$$

According to eqns (1) and (2), it follows that

$$\rho_s = \frac{1 + \mathring{\varepsilon}_s(s)}{\dfrac{\mathrm{d}\theta}{\mathrm{d}s} + \dfrac{\mathrm{d}\varphi}{\mathrm{d}s}} \tag{5b}$$

Moreover, the undeformed length $dl$ of a circumferential fibre at $(s,t)$ becomes $dl^*$ after deformation, and can be written as

$$dl = ds\left(1 + \frac{d\theta}{ds}t\right)$$

and

$$dl^* = (1 + \mathring{\varepsilon}_s)\,ds\left(1 + \frac{t}{\rho_s}\right)$$

respectively. These give

$$\varepsilon_s(s,t) = \frac{dl^* - dl}{dl} = \left(\mathring{\varepsilon}_s + t\frac{d\varphi}{ds}\right)\Big/\left(1 + t\frac{d\theta}{ds}\right) \tag{6}$$

Thus, the strain energy of a tube per unit length can be expressed as

$$U = 2\int_{s_1}^{s_2}\int_{-T/2}^{T/2}\left(\int_0^{\varepsilon_z^F}\sigma_z\,d\varepsilon_z + \int_0^{\varepsilon_s^F}\sigma_s\,d\varepsilon_s\right)dt\,ds \tag{7}$$

where $\sigma_z$ and $\sigma_s$ are the stress components in the $z$ and $s$ directions, respectively; $T$ is the thickness of the tube wall; and $\varepsilon_z^F$ and $\varepsilon_s^F$ are the final strain values of $\varepsilon_z$ and $\varepsilon_s$, respectively.

In the above derivations, shear deformation is omitted and this will be held throughout our investigation.

As it has been assumed that possible local unloading in the tube wall during deformation is ignored, the constitutive equation of the material of the tube can then be written as

$$\bar{\sigma} = \sigma_0\bar{\varepsilon}^n \tag{8}$$

where $\bar{\sigma}$ and $\bar{\varepsilon}$ are the effective stress and effective strain, respectively; $\sigma_0$ is a proportional factor and $n$ is a constant of the material. Hence,

$$\bar{\sigma}/\bar{\varepsilon} = \sigma_0\bar{\varepsilon}^{n-1} \tag{9}$$

and the deformation theory yields

$$\sigma_z = \frac{2}{9}\sigma_0\bar{\varepsilon}^{n-1}(2\varepsilon_z - \varepsilon_s) + \frac{E}{3(1-2\nu)}(\varepsilon_z + \varepsilon_s) \tag{10a}$$

$$\sigma_s = \frac{2}{9}\sigma_0\bar{\varepsilon}^{n-1}(2\varepsilon_s - \varepsilon_z) + \frac{E}{3(1-2\nu)}(\varepsilon_z + \varepsilon_s) \tag{10b}$$

where $E$ is Young's modulus, $\nu$ is Poisson's ratio, and

$$\bar{\varepsilon} = \frac{2}{3}(\varepsilon_z^2 + \varepsilon_s^2 - \varepsilon_z\varepsilon_s)^{1/2} \tag{11}$$

Therefore, eqn (7) gives

$$U = 2\int_{s_1}^{s_2}\int_{-T/2}^{T/2}(\omega_1 + \omega_2)\,\mathrm{d}t\,\mathrm{d}s \tag{12}$$

where

$$\omega_1 = \frac{2}{9}\sigma_0\int_0^{\varepsilon_z}\bar{\varepsilon}^{n-1}(2\varepsilon_z - \varepsilon_s)\,\mathrm{d}\,\varepsilon_z + \int_0^{\varepsilon_z}\bar{\varepsilon}^{n-1}(2\varepsilon_s - \varepsilon_z)\,\mathrm{d}\,\varepsilon_s \tag{13a}$$

$$\omega_2 = \frac{E}{6(1-2\nu)}(\varepsilon_z + \varepsilon_s)^2 + 2\varepsilon_z\varepsilon_s \tag{13b}$$

in which, for the sake of convenience, $\varepsilon_i^{\mathrm{F}}\,(i = z, s)$ have been replaced by $\varepsilon_i\,(i = s, z)$, respectively.

Assuming that there is no elongation on the middle surface of the tube circumferentially, i.e. only the bending strain of $\varepsilon_s$ is considered, we have

$$\mathring{\varepsilon}_s = 0$$

Moreover, we only discuss a moderately thin-walled tube which has the following properties:

$$\mathring{\varepsilon}_z \gg \left|\frac{t}{\rho_z}\sin(\theta + \varphi)\right|$$

$$\left|t\frac{\mathrm{d}\theta}{\mathrm{d}s}\right| \ll 1$$

Thus eqns (4) and (6) can be simplified to

$$\varepsilon_z = \mathring{\varepsilon}_z \tag{14a}$$

$$\varepsilon_s = t\frac{\mathrm{d}\varphi}{\mathrm{d}s} \tag{14b}$$

respectively.

As a special case, we analyze an originally circular tube with radius $R$ of the middle surface. Considering the second of the four experimental observations listed in the Introduction, let the displacement component normal to the middle surface (see Figs 3 and 4) be

$$w = R\zeta\cos 2\psi \tag{15}$$

where $\zeta$ is a dimensionless parameter which expresses the severity of flattening of the cross-section of the tube and is called the *flattening ratio*; $\psi$ is an angle shown in Fig. 4. Thus, the variation of the circumferential curvature during deformation can now be expressed as

$$\frac{\mathrm{d}\varphi}{\mathrm{d}s} = \frac{3\zeta}{R}\cos 2\psi \tag{16}$$

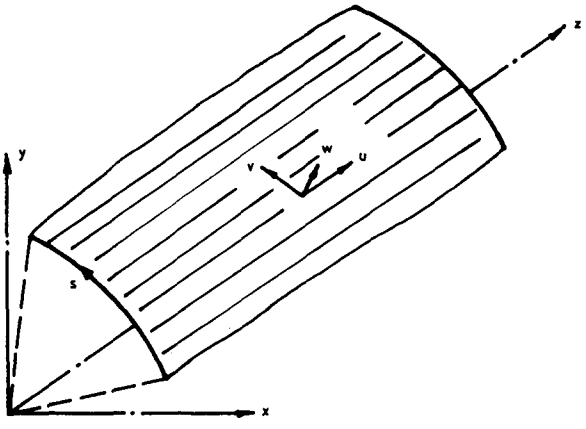


**Fig. 3.** The displacements on the middle surface.

The substitutions of eqn (16) into eqns (14) and then into eqn (12) yield the expression of strain energy $U$ in terms of $\zeta$. By noting that the variation of $\zeta$ makes $U$ take a minimum, it is obvious that

$$\frac{\partial U}{\partial \zeta} = 0 \tag{17}$$

Accordingly, the bending moment is determined by

$$M = \frac{\partial U}{\partial K} \tag{18}$$

where $K = 1/\rho_z$ is the axial curvature.

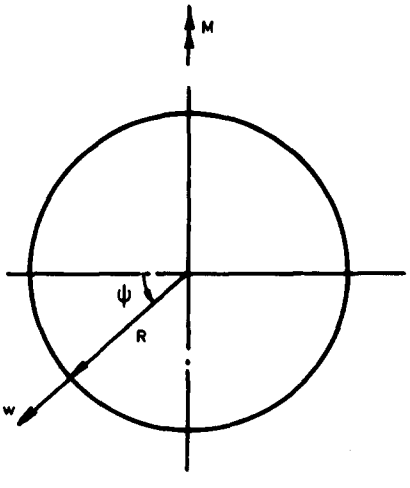


**Fig. 4.** The middle surface of an originally circular tube.

Keeping eqn (15) in mind, the current flow area, $A_f$, of the tube can then be calculated by simple integration after $\zeta$ has been obtained from eqn (17). Thus the area ratio, $A_f/A_0$, is obtained, where $A_0 = \pi(R - T/2)^2$ is the original flow area of the tube.

## A NUMERICAL EXAMPLE

To examine the above analyses, an example given by Ref. 9 is calculated by the present method numerically. The constitutive equation is taken to be

$$\bar{\sigma} = 895\bar{\varepsilon}^{0.26}$$

and Young's modulus and the geometrical parameters are $E = 2{\cdot}08 \times 10^5\,\mathrm{N\,mm^{-2}}$, $R = 33{\cdot}3\,\mathrm{mm}$ and $T = 9{\cdot}5\,\mathrm{mm}$, respectively. Table 1

**TABLE 1**
Relationship between $K$ and $\zeta$

| *No.* | $K\,(m^{-1})$ | $\zeta$ |
|---|---|---|
| 1 | 0·1 | 0·002 9 |
| 2 | 0·2 | 0·007 1 |
| 3 | 0·3 | 0·013 1 |
| 4 | 0·4 | 0·020 2 |
| 5 | 0·5 | 0·029 9 |
| 6 | 0·6 | 0·038 8 |
| 7 | 0·7 | 0·051 9 |
| 8 | 0·8 | 0·070 3 |
| 9 | 0·9 | 0·091 0 |
| 10 | 1·0 | 0·112 7 |
| 11 | 1·7 | 0·269 2 |
| 12 | 2·5 | 0·473 2 |
| 13 | 5·0 | 0·855 6 |

shows the values of the dimensionless parameter $\zeta$ with the variation of curvature $K$. Figure 5 displays the relationship between $K$ and $\zeta$ directly. In this figure, the dotted curve is the enlargement of segment $\widehat{OA}$ in the solid curve. It can be seen from Fig. 5 that $\zeta$ varies very slowly at the beginning of deformation and increases severely when $0{\cdot}5\,\mathrm{m^{-1}} \leq K \leq 1{\cdot}5\,\mathrm{m^{-1}}$, and then varies very slowly again after $K \geq 4\,\mathrm{m^{-1}}$. The upper curve in Fig. 6 shows the case of decreasing flow area, $A_f$, of the tube with increasing curvature $K$. It follows that this curve is similar to the $\zeta$–$K$ curve of Fig. 5 if the latter is reversed about a horizontal axis. It also shows that when $A_f$ becomes smaller

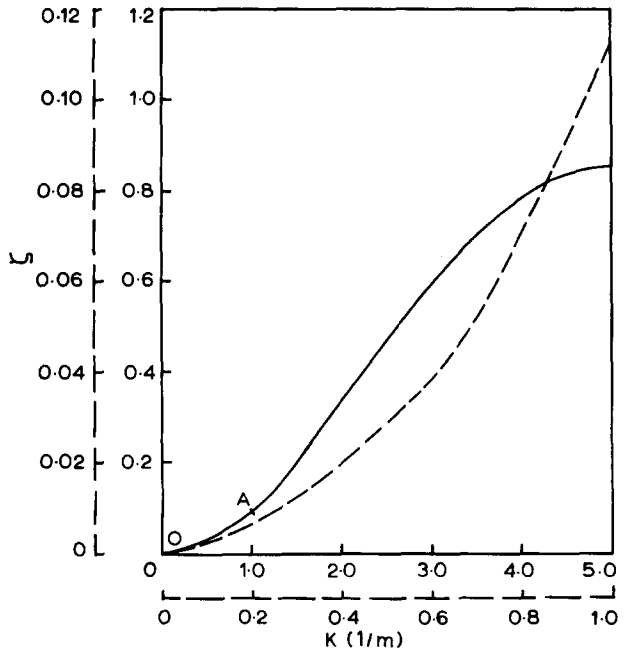


**Fig. 5.** Curve of $\zeta$–$K$.

and smaller, the upper and lower parts of the inner surface of the tube nearly touch each other at this time. The variation of bending moment shown by the lower curve in Fig. 6 indicates that the load-carrying capacity of the tube first increases and then decreases and finally reaches a constant value. It can also be seen that the maximum value of the bending moment is at $K = 1{\cdot}4\,\mathrm{m}^{-1}$.

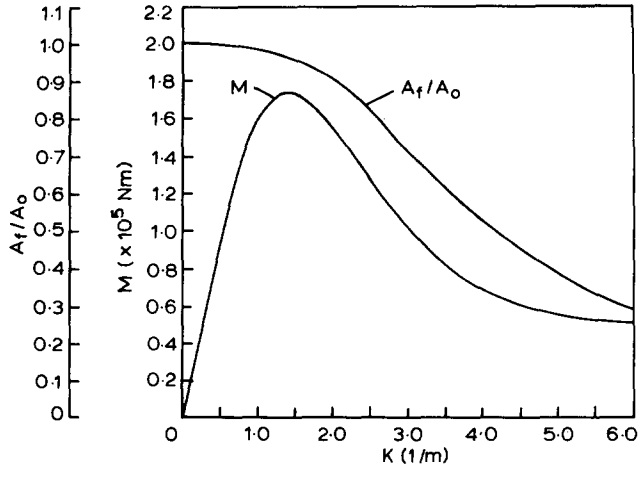


**Fig. 6.** Curves of $M$–$K$ and $A_f/A_0$–$K$.

## CONCLUSIONS

The results on the variations of flattening ratio and bending moment obtained by the present method are in good accordance with those reported by experiments.[6-9] The procedure of the present analyses is simple, straightforward and convenient. Numerical results show that the flow area decreases rapidly with increment of flattening ratio of the cross-section, and this would give an advantage in controlling a rupture accident of a pipeline in chemical and nuclear power plants.

However, the investigation reported in this paper is preliminary. The effects of many factors, such as the inner pressure, the local unloading and so on, are ignored, since the focus of attention at present is to facilitate the engineering application. It is expected that these considerations will be the subject of further projects by the authors.

## REFERENCES

1. Brazier, L. G., On flexure of thin cylindrical shells and other thin sections. *Proc. R. Soc. Lond., Ser. A*, **116** (1927) 104–14.
2. Reissner, E., On finite pure bending of cylindrical tube, *Österr. Ing. Arch.*, **15** (1961) 165–72.
3. Seide, P. and Weingarten, V. I., On the buckling of circular cylindrical shells under pure bending, *J. Appl. Mech.*, **28** (1961) 112–16.
4. Yu, T. X. and Hua, Y. L., The whipping during pipe rupture accident and its defence in nuclear power plant, *Pressure Vessel Tech.*, **3** (1986) 70–6 (in Chinese).
5. Gerber, T. L., Plastic deformation of piping due to pipe-whip loading, ASME paper 74-NE-1.
6. Belke, L., A simple approach for failure bending moments of straight pipes, *Nucl. Engng Des.*, **77** (1984) 1–5.
7. Prinja, N. K. and Chitkara, N. R., Post-collapse cross-sectional flattening of thick pipes in plastic bending, *Nucl. Engng Des.*, **83** (1984) 113–21.
8. Ueda, S., Moment–rotation relationship considering flattening of pipe due to pipe whip loading, *Nucl. Engng Des.*, **85** (1985) 251–9.
9. Prinja, N. K., Parker, J. V. and Day, B. V., The large strain–large displacement behaviour of a whipping pipe, *Proc. I. Mech. E.* (1985) 225–34.